Apratoxin D, a Potent Cytotoxic Cyclodepsipeptide from Papua New Guinea Collections of the Marine Cyanobacteria *Lyngbya majuscula* and *Lyngbya sordida*

Marcelino Gutiérrez,[†] Takashi L. Suyama,[†] Niclas Engene,[†] Joshua S. Wingerd,[†] Teatulohi Matainaho,[‡] and William H. Gerwick*,[†]

Center for Marine Biotechnology and Biomedicine, Scripps Institution of Oceanography and Skaggs School of Pharmacy and Pharmaceutical Sciences, University of California at San Diego, La Jolla, California 92093, and Discipline of Pharmacology, School of Medicine and Health Sciences, University of Papua New Guinea, National Capital District, Papua New Guinea

Received February 23, 2008

Cancer cell toxicity-guided fractionation of extracts of the Papua New Guinea marine cyanobacteria *Lyngbya majuscula* and *Lyngbya sordida* led to the isolation of apratoxin D (**1**). Compound **1** contains the same macrocycle as apratoxins A and C but possesses the novel 3,7-dihydroxy-2,5,8,10,10-pentamethylundecanoic acid as the polyketide moiety. The planar structures and stereostructures of compound **1** were determined by extensive 1D and 2D NMR and MS data analyses and by comparison with the spectroscopic data of apratoxins A and C. Apratoxin D (**1**) showed potent in vitro cytotoxicity against H-460 human lung cancer cells with an IC_{50} value of 2.6 nM.

Apratoxins A−C (**2**−**4**) are a fascinating group of cyclodepsipeptides of mixed biosynthetic origin possessing both peptide and polyketide segments. Members of this compound family show potent in vitro cytotoxicity against the KB (0.52−21.3 nM) and LoVo cell lines (0.36−10.8 nM).[1,2] Efforts to elucidate the mechanism of action of apratoxin A revealed that this compound induces G_1-phase cell-cycle arrest and apoptosis.[3] Three total syntheses of apratoxin A (**2**) have been reported by the groups of Forsyth,[4] Takahashi,[5] and Liu,[6] and, from the latter effort, in which four oxazoline analogues of apratoxin A were synthesized, it was found that replacement of the thiazoline ring with an oxazoline ring had only a marginal effect on potency. Furthermore, this same study also established that the two methyl groups at C-37 and C-40 as well as the stereochemistry at C-37 were essential for cellular inhibitory activity of these apratoxin analogues.[6]

To date, apratoxins have been isolated only from *Lyngbya* species collected in Guam and Palau.[1,2] At the time of the initial report of apratoxin A, we had isolated and defined this same molecular structure from a Papua New Guinea collection of *Lyngbya bouillonii* (Tan and Gerwick, unpublished). Recently, we have reisolated apratoxins A−C (**2**−**4**) from yet another collection of *L. bouillonii* from Papua New Guinea and established unicyanobacterial cultures in the laboratory that produce the apratoxins.

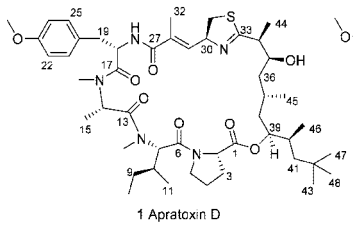

1 Apratoxin D

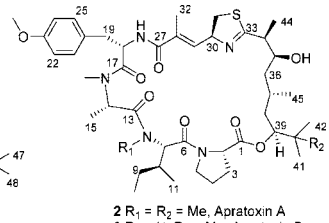

2 $R_1 = R_2 =$ Me, Apratoxin A
3 $R_1 =$ H, $R_2 =$ Me, Apratoxin B
4 $R_1 =$ Me, $R_2 =$ H, Apratoxin C

Herein, we report the isolation and structural determination of a new member of the apratoxin family, apratoxin D (**1**), obtained from collections of two other species of cyanobacteria, *L. majuscula* (Oscillatoriaceae, Harvey ex Gomont 1892) and *L. sordida* (Oscillatoriaceae, Gomont ex Gomont 1892), both collected in Papua New Guinea. Structural analysis showed that compound **1** has the same sequence of amino acid residues as apratoxins A and C, but contains a new polyketide moiety, 3,7-dihydroxy-2,5,8,10,10-pentamethylundecanoic acid, which is longer than that in the other apratoxins by an acetate group. Inclusion of this polyketide chain into an apratoxin structure has intriguing biosynthetic implications and provides additional insights into the necessary structural features for potent biological activity in this structural class. Pure apratoxin D (**1**) showed potent cytotoxicity against H-460 lung cancer cells (IC_{50} 2.6 nM).

The marine cyanobacteria *L. majuscula* and *L. sordida* were collected by hand using scuba from New Ireland and Pigeon Island in Papua New Guinea. Both species were separately extracted and prefractionated to obtain nine fractions that were evaluated for cytotoxicity. Fraction H from both species, eluting with 25% MeOH/EtOAc, produced 70−82% mortality at 1 ppm in the brine shrimp lethality assay and showed significant cytotoxicity to H-460 human lung cancer cells (80% toxicity at 5 μg/mL). Further purification of this bioactive material using reversed-phase HPLC eluted with a MeOH/H_2O gradient, yielded 1.9 and 1.0 mg of apratoxin D (**1**), respectively, from *L. majuscula* and *L. sordida*.

Compound **1** was optically active ($[\alpha]_D$ −95.1 (*c* 0.13, MeOH)) and gave an $[M + H]^+$ ion at *m*/*z* 882.5395 by HRESI-TOFMS, for a molecular formula of $C_{48}H_{76}N_5O_8S$. In $CDCl_3$, apratoxin D displayed well-dispersed ^1H and ^{13}C NMR spectra, although only 43 carbon resonances were observed. However, this reduced number of carbon signals was attributable to two degenerate carbonyl signals at δ_C 170.5 and several elements of localized symmetry giving larger than expected carbon peaks for the methyl groups of a tertiary butyl function (δ_H 0.89, 9H, s; δ_C 30.0), and the protonated carbons of a 1,4-disubstituted aromatic ring [δ_H 7.15 (2H, d, J = 9.0 Hz), 6.79 (2H, d, J = 9.0 Hz); δ_C 130.6, 113.9], thus accounting for all 48 carbon atoms. Other signals in the ^1H and ^{13}C NMR spectra, such as one ester and four amide-type carbonyls (δ169.6−172.7), a series of midfield signals consistent with α-amino protons and carbons, and two *N*-methyl groups, indicated that compound **1** is substantially composed of amino acid subunits. Additionally, there were two proton resonances that showed no correlations to any carbon atoms by HSQC, and on the basis of their chemical shifts, were consistent with an amide proton (δ_H 6.12, 1H, d, J = 9.5 Hz) and a hydroxyl proton (δ_H 4.66, 1H, d, J = 11.0 Hz). Another distinctive feature of the ^1H NMR spectrum of **1** was the occurrence of a relatively large number of methyl groups, 13 in total (nine at high field, one olefinic, two *N*-methyls as described above, and an *O*-methyl group at δ_H 3.78, 3H, s).

* To whom correspondence should be addressed. Tel: (858) 534-0578. Fax: (858) 534-0529. E-mail: wgerwick@ucsd.edu.
[†] University of California at San Diego.
[‡] University of Papua New Guinea.

10.1021/np800121a CCC: $40.75 © 2008 American Chemical Society and American Society of Pharmacognosy
Published on Web 04/30/2008

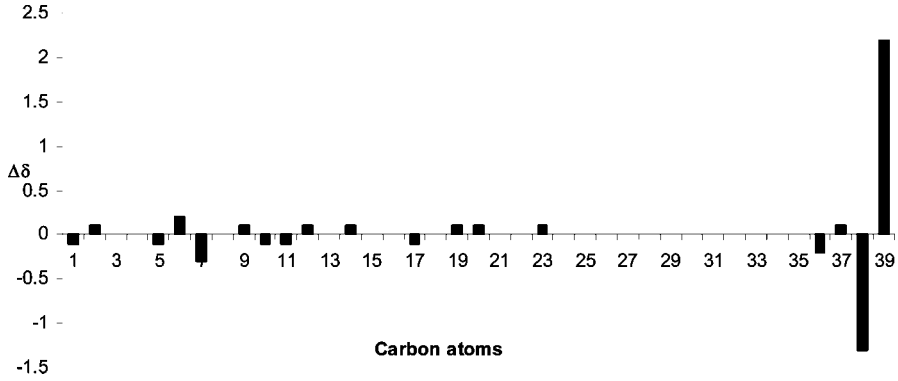

Figure 1. $\delta\Delta_C$ of apratoxins D (**1**) and A (**2**).

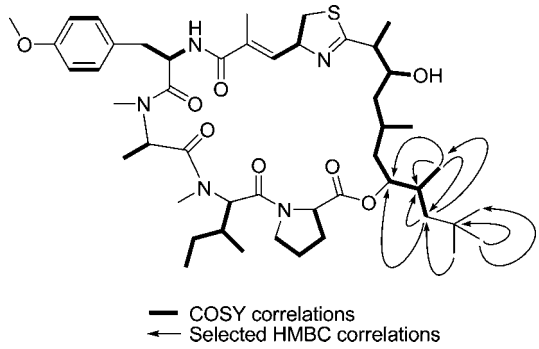

Figure 2. Selected 2D NMR correlations for the polyketide unit in apratoxin D (**1**).

Comparison of this data set with marine cyanobacterial lipopeptides reported in the literature, especially the *tert*-butyl functionality, which is known in only a few cases (apratoxins,[1,2] antillatoxins A[7] and B,[8] madangolide,[9] laingolide,[10] and ypaoamide[11]), identified a close fit with apratoxin A (**2**). Indeed, a careful comparison of ^{1}H and ^{13}C NMR chemical shifts, as well as ^{1}H−^{1}H coupling constants, between compound **1** and apratoxin A showed them to be identical through the majority of the structure. The only significant variations in chemical shifts between the two compounds were localized to the terminus of the lipid chain, specifically at the shifts for C-38 and C-39 ($\Delta\delta_{C\text{-}38}$ = 1.3 ppm, $\Delta\delta_{C\text{-}39}$ = 2.2 ppm; Figure 1 and Supporting Information). In combination with the 42 mass unit difference (C_3H_6) between the two compounds, we deduced that compound **1** is a homologue of apratoxin A, and by HSQC, contained additional secondary methyl, methylene, and methine groups. The positions of these three new carbon atoms were defined through HSQC, COSY, and HMBC experiments. The proton at H-39 was adjacent to a methine at δ 1.63, which was, in turn, coupled to both a methyl group (δ 0.93) and the diasterotopic protons of a methylene (δ 1.28 and 0.92). This latter methylene was located adjacent to the *tert*-butyl group through a series of reciprocal HMBC correlations. Hence, the complete spin system of a new 3,7-dihydroxy-2,5,8,10,10-pentamethylundecanoic acid unit was clearly defined from a combination of COSY and HMBC data (Figure 2).

The relative configuration of the chiral centers around the macrocycle (C-1 to C-39) could be assigned as the same as in apratoxin A (**2**) on the basis of the closely similar chemical shifts and coupling constants. Moreover, because the optical rotation of apratoxin A and the new compound, apratoxin D (**1**), were both strongly negative (**1**, $[\alpha]_D$ −95.1; **2**, $[\alpha]_D$ −161), they are likely of the same enantiomeric series. The relative configuration of the remaining chiral center, C-40, with respect to C-39 was determined on the basis of *J*-based configurational analysis,[12] ROESY correlations, and molecular modeling. A $^3J_{HH}$ coupling constant of 4.0 Hz between H-39 and H-40 indicated that these protons were in a

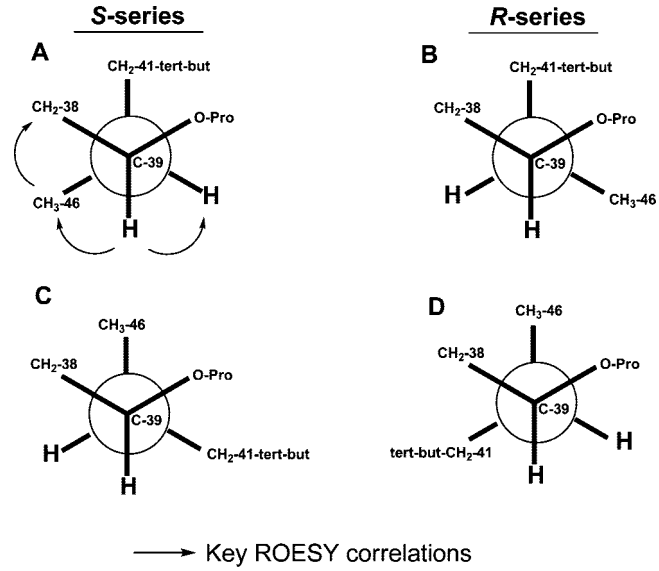

Figure 3. Possible conformations for *R** and *S** configurations at C-40 of apratoxin D (**1**).

gauche orientation. Therefore, the only possible conformers for the 40*S** stereoisomer were rotamers A and C, whereas those for the 40*R** stereoisomer were rotamers B and D, respectively (Figure 3). Ab initio geometry optimization of each of the four conformers revealed that A is 3.66 kcal/mol more stable than C and that B is 0.84 kcal/mol more stable than D. On the basis of NOE correlations observed from CH_3-46 to CH_2-38 and CH-39 of apratoxin D (**1**) (Figure 3), the relative stereochemistry at C-40 could be assigned as 40*S**, as depicted for conformer A.

In in vitro assays, apratoxin D (**1**) showed an IC_{50} of 2.6 nM against H-460 human lung cancer cells. This is nearly equipotent to that of apratoxin A (**2**) and, hence, indicates that the activity of the drug is not strongly impacted by the larger lipopeptide tail. This could be important to the design of analogue structures for probing the mechanism of action of the apratoxins. For example, the polyketide terminus may be a suitable location at which to attach linkers for biotinylation or fluorescent probes. Biosynthetically, the occurrence of an apratoxin-type metabolite that is chain elongated in this section of the molecule suggests that either (a) apratoxins A−C (**2**−**4**) are produced by the same genetic pathway, however, with skipping of this PKS and methyl transferase module, or (b) apratoxin D (**1**) is produced by a new biosynthetic pathway that contains the additional genetic elements for one more PKS extension, methylation by SAM, and full ketone reduction at C-41. In this regard, it is interesting that we isolated this new member of the apratoxin family from two distinct species of the genus *Lyngbya*, and this finding supports the hypothesis that genetic transfer of natural product biosynthetic pathways between different marine

Table 1. NMR Spectroscopic Data (500 MHz, $CDCl_3$) for Apratoxin D (**1**)

position	δ_C, mult.	δ_H (J in Hz)	HMBC[a]
Pro			
1	172.7, qC		
2	59.7, CH	4.16, t (7.6)	1, 3, 4
3a	29.3, CH_2	1.89, m	1, 4, 5
3b		2.21, m	
4a	25.6, CH_2	1.87, m	2
4b		2.07, m	
5a	47.7, CH_2	3.66, m	2, 3, 4
5b		4.18, m	
N-Me-Ile			
6	170.5, qC		
7	56.9, CH	5.18, d (12.0)	6, 8, 9, 11, 12, 13
8	31.8, CH	2.21, m	
9a	24.6, CH_2	0.93, m	
9b		1.32, m	
10	9.1, CH_3	0.91, d (7.0)[b]	7, 8, 9
11	14.1, CH_3	0.92, d (6.0)[b]	8, 9
12	30.4, CH_3	2.69, s	7, 13
N-Me-Ala			
13	170.0, qC		
14	60.6, CH	3.29, bq (6.5)	15, 17
15	13.9, CH_3	1.21, d (6.5)	13, 14
16	36.7, CH_3	2.81, s	14, 17
O-Me-Tyr			
17	170.5, qC		
18	50.5, CH	5.05, m	19, 20
19a	37.1, CH_2	2.86, dd (12.6, 4.8)	18, 20, 21, 25
19b		3.12, m	
20	128.2, qC		
21/25	130.6, CH	7.15, (9.0)	19, 21, 22, 23, 25
22/24	113.9, CH	6.79, (9.0)	20, 22, 23, 24
23	158.6, qC		
26	55.3, CH_3	3.78, s	23
NH		6.12, d (9.5)	27
MoCys			
27	169.6, qC		
28	130.5, qC		
29	136.3, CH	6.34, dd (10.0, 1.0)	27, 31, 32
30	72.5, CH	5.24, dt (10.0, 8.8, 4.3)	28, 29, 33
31a	37.6, CH_2	3.13, dd (10.9, 4.3)	29, 30
31b		3.46, dd (10.9,8.8)	
32	13.3, CH_3	1.95, d (1.0)	27, 28, 29
polyketide			
33	177.4, qC		
34	49.1, CH	2.63, dq (9.5, 7.0)	33, 35, 44
35	71.6, CH	3.55, dddd (11.4, 11.0, 9.5, 3.3)	
36a	38.3, CH_2	1.11, m	
36b		1.53, ddd (14.0, 11.4, 4.5)	
37	24.2, CH	2.18, m	
38a	39.0, CH_2	1.20, m	
38b		1.79, ddd (14.0, 12.5, 3.0)	
39	75.2, CH	5.02, ddd (12.5[b], 4.0, 2.5)	1, 41
40	33.9, CH	1.63, m	39, 41, 46
41a	46.0 CH_2	1.28, m	39, 40, 43, 46, 47, 48
41b		0.92, m	
42	31.9, qC		
43	30.0, CH_3	0.89, s	41, 42
44	16.6, CH^3	1.07, d (7.0)	33, 34, 35
45	19.7, CH_3	0.98, d (7.0)	37
46	18.4, CH_3	0.93, d (6.0)[b]	39, 40, 41
47	30.0, CH_3	0.89, s	41, 42, 43
48	30.0, CH_3	0.89, s	41, 42, 43
OH		4.66, d (11.0)	35, 36

[a] HMBC correlations are from proton(s) stated to the indicated carbon. [b] J_{HH} calculated from the HSQC spectra.

cyanobacteria is common.[13] Currently, we are examining the biosynthetic pathway to the apratoxins via complementary gene cloning and genome sequencing strategies, and we hope to gain insight into this intriguing question.

Experimental Section

General Experimental Procedures. Optical rotations were measured with a JASCO P-2000 polarimeter. IR spectra were recorded on a Nicolet IR 100 FT-IR spectrophotometer, and UV spectra were measured on a Beckman Coulter DU-800 spectrophotometer. NMR spectra were acquired on Varian Inova 500 and 300 MHz spectrometers and referenced to residual solvent ^1H and ^{13}C signals (δ_H 7.26, δ_C 77.0 for $CDCl_3$). Low-resolution ESIMS were acquired on a Finnigan LCQ Advantage Max mass spectrometer, while high-accuracy mass measurements were obtained on an Agilent ESI-TOF mass spectrometer. Purification of the compounds was carried out on a Waters HPLC system equipped with a Waters 515 binary pump, a Waters 996 PDA detector, and a Phenomenex Jupiter C_{18} column (10 μm, 10 $\times$ 250

mm). The morphological characterization of OSC3L was performed using an Olympus BH-2 light microscope.

Biological Material Collection and Identification. The marine cyanobacterium *Lyngbya majuscula* was collected from a depth of 15 m from New Ireland in Papua New Guinea (S 3°49.626′, E 152°26.017′). The *L. sordida* sample was collected from a depth of 9 m from Pigeon Island in Papua New Guinea (S 4°16.063′, E 152°20.266′). The samples were stored in 1:1 EtOH/H_2O and frozen at −20 °C. Voucher specimens are available from WHG as collection number PNG 5-22-05-3 for *L. majuscula* and PNG 5-19-05-4 for *L. sordida*.

Morphological Characterization. Morphological identification was made in accordance with traditional phycological[14,15] and bacteriological systems.[16] The two *Lyngbya* strains PNG5-194 and PNG5-223 were identified morphologically as *L. sordida* (Gomont ex Gomont 1892) and *L. majuscula* (Harvey ex Gomont 1892), respectively. Macroscopically, *L. sordida* PNG5-194 and *L. majuscula* PNG5-223 were relatively similar in their thallus appearance, and both grew as brown-red mats covering the reef substrates. However, on a cellular level, the two strains were distinct from each other. *L. sordida* PNG5-194 had cylindrical filaments, 57 μm wide and with distinct sheaths. The discoid cells were wide (44 μm wide and 15 μm long) and with constrictions at cross-walls. The end cells were rounded, noncapitated, and without the presence of calyptras. The filaments of *L. majuscula* PNG5-223 were also cylindrical, with distinct sheaths and approximately the same size (56 μm in width). The cells were disk-shaped (47 μm wide and 2.5 μm long), but distinctively much thinner with cell length/width ratios of 0.05 compared with 0.3 of *L. sordida* PNG5-194. *L. majuscula* PNG5-223 also differed from *L. sordida* PNG5-194 in the absence of constrictions at the cross-walls. The end cells were also rounded, noncapitated, and did not contain calyptras.

Molecular−Phylogenetic Analysis. Partial 16S rRNA gene sequences of *L. sordida* PNG5-194 and *L. majuscula* PNG5-223 were PCR-amplified and sequenced. The 16S rRNA gene sequence of *L. sordida* PNG5-194 included 1376 nucleotides, or ∼95% of the gene coverage (GenBank acc. no. EU492877), and *L. majuscula* PNG5-223 included 952 nucleotides, or ∼66% of the gene coverage (GenBank acc. no. EU492878). On the basis of the 16S rRNA gene sequence identities, the two strains are very closely related, with a sequence divergence of 0.9%. A BLAST search combined with a phylogenetic analysis revealed a cluster of *Lyngbya* species as the phylogenetically closest related organisms. Interestingly, *L. sordida* PNG5-194 showed 100% sequence identity with the strain *Lyngbya* sp. NIH309 (GenBank acc. no. AY049752) from Guam, while *L. majuscula* PNG5-223 showed highest sequence identity (99.6%) with *Lyngbya* sp. VP417a from Palau (GenBank acc. no. AY049750).

DNA Extraction, 16S rRNA Gene PCR-Amplification, and Cloning. Genomic DNA was extracted from 40 mg of clean algae tissue using the Wizard Genomic DNA purification kit (cat. A1120) according to the manufacturer's specifications (Promega, Madison, WI). The isolated genomic DNA was further purified using a Genomic-tip 20/G from Qiagen (cat. 10223). The 16S rRNA gene was amplified from isolated DNA using the cyanobacteria-specific primers 106F and 1509R, as previously described.[17] The reaction volume was 25 μL containing 0.5 μL of DNA (50 ng), 2.5 μL of 10 × PfuUltra II reaction buffer, 0.5 μL of dNTP mix (25 mM each of dATP, dTTP, dGTP, and dCTP), 0.5 μL of each primer (10 μM), 0.5 μL of PfuUltra II fusion HS DNA polymerase (cat. 600760), and 20.25 μL of dH_2O. The PCR reaction was performed in an Eppendorf Mastercycler gradient as follows: initial denaturation for 2 min at 95 °C, 30 cycles of amplification (20 s at 95 °C, 20 s at 50 °C, and 15 s at 72 °C), and final elongation for 3 min at 72 °C. PCR products were subcloned, with the Zero Blunt TOPO PCR cloning kit (cat. K2800-20SC) from Invitrogen, into pCR-Blunt II TOPO vector, transformed into TOPO cells, and cultured on LB-Kanamycin plates. Plasmid DNA was isolated using the QIAprep spin miniprep kit (cat. 27106) from Qiagen and sequenced with pCR-Blunt II TOPO vector-specific primers M13F/M13R and internal middle primers 359F and 781R as previously described.[17]

Phylogenetic Analysis. The bidirectional 16S rRNA gene sequences of *L. sordida* PNG5-194 and *L. majuscula* PNG5-223 were individually combined in MEGA 4, and the resulting consensus sequence was inspected visually.[18] The 16S rRNA genes were phylogentically compared with related sequences using the nBLAST analysis tool and the phylogenetic trees created by Tree View, both available at NCBI's home page (http://www.ncbi.nih.gov).

Extraction and Isolation. *L. majuscula* was extracted with 2:1 CH_2Cl_2/MeOH and concentrated to dryness in vacuo to give 980 mg of crude extract. VLC prefractionation of the crude extract using a gradient with 0−100% EtOAc in hexanes followed by 0−100% of MeOH in EtOAc yielded nine fractions (A−I). Fraction H, eluted with 25% MeOH in EtOAc (125 mg), showed potent toxicity against brine shrimp and H-460 lung cancer cells and was further purified by reversed-phase HPLC (continuous gradient from 60:40 MeOH/H_2O to 100% MeOH in 65 min at 2 mL/min) to give 1.9 mg of apratoxin D (**1**) as a pale yellow, amorphous powder. The same protocol as above yielded 1.0 mg of apratoxin D from *L. sordida*.

Apratoxin D (1): pale yellow, amorphous powder $[\alpha]^{25}_D$ −95.1 (*c* 0.13, MeOH); UV (MeOH) λ_{max} (log ϵ) 201 (3.94), 226 (3.73) nm; IR (film) ν_{max} 3364 (br), 2922, 2852, 1737, 1625, 1512, 1461, 1356, 1248, 1181 cm^{-1}; ^1H and ^{13}C NMR, see Table 1; ESIMS *m/z* 882 (100) $[M + H]^+$, 904 (6) $[M + Na]^+$, 1763 (41) $[2\ M + H]^+$; HRESI-TOFMS *m/z* $[M + H]^+$ 882.5395 (calcd for $C_{48}H_{76}N_5O_8S$, 882.5409).

Biological Activity. Brine shrimp (*Artemia salina*) toxicity was measured as previously described.[19] After a 24 h hatching period, aliquots of 10 mg/mL stock solutions of sample were added to test wells containing 5 mL of artificial seawater and brine shrimp to achieve a range of final concentrations from 0.1 to 100 ppm. After 24 h the live and dead shrimp were tallied.

Cytotoxicity was measured in NCI H-460 human lung tumor cells with cell viability being determined by MTT reduction.[20] Cells were seeded in 96-well plates at 6000 cells/well in 180 μL of medium. After 24 h, the test chemicals were dissolved in DMSO and diluted into medium without fetal bovine serum and then added at 20 μg/well. DMSO was less than 0.5% of the final concentration. After 48 h, the medium was removed and cell viability determined.

Conformer Distribution Calculations and ab Initio Geometry Optimization. Spartan '04 (Wavefunction, Inc., Irvine, CA) was used for all molecular modeling calculations. Conformers A through D were identified and obtained through a conformer distribution calculation using molecular mechanics. The geometry of each conformer was optimized by Hartree−Fock 3-21G* ab initio calculations. Hartree−Fock 3-21G* single-point energy calculation was used to obtain the absolute energy of each conformer for comparison.

Acknowledgment. We gratefully acknowledge the government of Papua New Guinea for permission to make these collections. M.G. thanks SENACYT, Panama, for financial support. We also thank C. Sorrels for help with collections. This work was supported by NIH CA 100851 and CA 52955.

Supporting Information Available: ^1H NMR, ^{13}C NMR, and 2D NMR spectra in $CDCl_3$ for apratoxin D (**1**); comparisons of the NMR data of apratoxin D (**1**) with apratoxins A and C. This material is available free of charge via the Internet at http://pubs.acs.org.

References and Notes

(1) Luesch, H.; Yoshida, W. Y.; Moore, R. E.; Paul, V. J. *Bioorg. Med. Chem.* **2002**, *10*, 1973–1978.

(2) Luesch, H.; Yoshida, W. Y.; Moore, R. E.; Paul, V. J.; Corbett, T. H. *J. Am. Chem. Soc.* **2001**, *123*, 5418–5423.

(3) Luesch, H.; Chanda, S. K.; Raya, R. M.; DeJesus, P. D.; Orth, A. P.; Walker, J. R.; Izpisua-Belmonte, J. C.; Schultz, P. G. *Nat. Chem. Biol.* **2006**, *2*, 158–167.

(4) Chen, J.; Forsyth, C. J. *J. Am. Chem. Soc.* **2003**, *125*, 8734–8735.

(5) Doi, T.; Numajiri, Y.; Munakata, A.; Takahashi, T. *Org. Lett.* **2006**, *8*, 531–534.

(6) Ma, D.; Zou, B.; Cai, G.; Hu, X.; Liu, J. O. *Chem.−Eur. J.* **2006**, *12*, 7615–7626.

(7) Orjala, J.; Nagle, D. G.; Hsu, V. L.; Gerwick, W. H. *J. Am. Chem. Soc.* **1995**, *117*, 8281–8282.

(8) Nogle, L. M.; Okino, T.; Gerwick, W. H. *J. Nat. Prod.* **2001**, *64*, 983–985.

(9) Klein, D.; Braekman, J. C.; Daloze, D.; Hoffmann, L.; Castillo, G.; Demoulin, V. *J. Nat. Prod.* **1999**, *62*, 934–936.

(10) Klein, D.; Braekman, J. C.; Daloze, D. *Tetrahedron Lett.* **1996**, *37*, 7519–7520.

(11) Nagle, D. G.; Paul, V. J.; Roberts, M. A. *Tetrahedron Lett.* **1996**, *37*, 6263–6266.

(12) Matsumori, N.; Kaneno, D.; Murata, M.; Nakamura, H.; Tachibana, K. *J. Org. Chem.* **1999**, *64*, 866–876.

(13) Simmons, T. L.; Coates, R. C.; Clark, B. R.; Engene, N.; Gonzalez, D.; Esquenazi, E.; Dorrestein, P. C.; Gerwick, W. H. *Proc. Natl. Acad. Sci., U.S.A.* **2008**, *105*, 4587−4594.
(14) Geitler, L. *L. Rabenhorst's Kryptogamen-Flora von Deutschland Österreich und der Schweiz*; Akademische Verlagsgesellschaft: Leipzig, 1932; pp 942−943.
(15) Komárek, J.; Anagnostidis, K. *Süsswasserflora von Mitteleuropa*; Spektrum Akademischer: Heidelberg, 2005; pp 576−579.
(16) Castenholz, R. W.; Rippka, R.; Herdman, M. In *Bergey's Manual of Systematic Bacteriology*; Garrity, G. M., Boone, D. R., Castenholz, R. W., Eds.; Springer: New York, 2001; Vol. 1, pp 492−553.
(17) Nubel, U.; Garcia-Pichel, F.; Muyzer, G. *Appl. Environ. Microbiol.* **1997**, *63*, 3327–3332.
(18) Tamura, K.; Dudley, J.; Nei, M.; Kumar, S. *Mol. Biol. Evol.* **2007**, *24*, 1596–1599.
(19) Meyer, B. N.; Ferrigni, N. R.; Putnam, L. B.; Jacobsen, L. B.; Nichols, D. E.; McLaughlin, J. L. *Planta Med.* **1982**, *45*, 31–33.
(20) Manger, R. L.; Leja, L. S.; Lee, S. Y.; Hungerford, J. M.; Hokama, Y.; Dickey, R. W.; Granade, H. R.; Lewis, R.; Yasumoto, T.; Wekell, M. M. *J. AOAC Int.* **1995**, *78*, 521–527.

NP800121A